

Secondary diphosphine and diphosphido ligands:
synthesis, characterisation and group 1
coordination compounds†Cite this: *Dalton Trans.*, 2014, **43**,
267Jamie S. Ritch,^{a,b} Delphine Julienne,^b Shayne R. Rybchinski,^b Kathryn S. Brockman,^b
Kevin R. D. Johnson^b and Paul G. Hayes^{*b}

Two types of secondary diphosphines, 1,8-(ArPH)₂C₁₄H₈ (**1a**: Ar = Tripp, 2,4,6-triisopropylphenyl; **1b**: Ar = Mes, 2,4,6-trimethylphenyl) and 1,3-(^tBuPHCH₂)₂C₆H₄ (**2**), based on rigid 1,8-anthracene and flexible *m*-xylyl frameworks, respectively, have been synthesized using different strategies. Compounds **1a** and **1b** were formed by nucleophilic aromatic substitution of a potassium organophosphido salt onto 1,8-difluoroanthracene, while compound **2** was obtained by addition of the Grignard reagent [1,3-(ClMgCH₂)₂C₆H₄]_x to a dichloroorganophosphine, followed by reduction to the diphosphine. These compounds were isolated as ca. 1 : 1 mixtures of *rac* and *meso* diastereomers as determined by multinuclear NMR spectroscopy. Borane and selenide derivatives of **2**, 1,3-(^tBuPH(BH₃)CH₂)₂C₆H₄ (**3**) and 1,3-(^tBuPH(Se)CH₂)₂C₆H₄ (**4**), were obtained. Preferential crystallization of one diastereomer of **3** and **4** was observed; X-ray crystallographic studies identified this as the *rac* isomer for diselenide **4**. Metallation studies of compounds **1a** and **2** yielded several alkali metal salts. The reaction of KH or K metal with **1a** yielded the compounds 1,8-(TrippPK)₂C₁₄H₈·xTHF (**5**) and 1,8-(TrippPK)₂C₁₄H₁₀·xTHF (**6**), respectively; in complex **6** the central aromatic ring has been reduced to yield a bent dihydroanthracene backbone. A crown ether derivative of **6**, [K(18-crown-6)(THF)₂][1,8-(TrippP)₂C₁₄H₁₀] (**7**), was characterised crystallographically. Double deprotonation of compound **2** with ⁷BuLi/TMEDA (TMEDA = *N,N,N',N'*-tetramethylethylenediamine) afforded the yellow dilithium complex 1,3-(^tBuPLiCH₂)₂C₆H₄·TMEDA (**8**), which crystallized as a dimer featuring lithium–arene π interactions.

Received 9th July 2013,
Accepted 1st October 2013
DOI: 10.1039/c3dt51844b

www.rsc.org/dalton

Introduction

The first tridentate pincer ligand was reported by Moulton and Shaw in the 1970s.¹ Since then, these compounds have grown in popularity as their late transition metal complexes find uses in homogeneous catalysis.² For example, the PCP iridium(III) dihydride complex [$\{2,6\text{-}(\text{}^t\text{Bu}_2\text{PCH}_2)_2\text{C}_6\text{H}_3\}\text{IrH}_2$] acts as a dehydrogenation catalyst *via* either transfer^{3a} or direct^{3b} processes, while the PNN ruthenium(II) hydride complex [$\{2\text{-}(\text{}^t\text{Bu}_2\text{PCH})\text{-}6\text{-}(\text{Et}_2\text{NCH}_2)\text{C}_5\text{H}_3\text{N}\}\text{Ru}(\text{CO})\text{H}$] catalyzes the formation of amides from primary amines and alcohols.⁴ Pincer ligands often impart to metal compounds increased solubility in organic solvents and high thermal stability (*e.g.* the complex

[$\{2,6\text{-}(\text{}^t\text{Bu}_2\text{PCH}_2)_2\text{C}_6\text{H}_3\}\text{NiCl}$] sublimes without decomposition at 240 °C).¹ Accordingly, metal complexes are often rendered suitable for reactivity and study under a wide variety of experimental conditions when supported by a pincer ligand.

In contrast to phosphine ancillaries such as the above-mentioned PCP or PNN pincers, multidentate ligands featuring anionic phosphido donors are much rarer. Examples of known di- and tri-phosphido compounds include $\{\text{Li}(\text{THF})_2\}\text{-}[\text{PhPCH}_2\text{CH}_2\text{PPh}]_2$,⁵ 1,2-(PhPLi)₂C₆H₄·2TMEDA,⁶ and $\{\text{MeC}(\text{CH}_2\text{PPhLi})_3\}\cdot 2\text{THF}\cdot \text{PMDTA}$ ⁷ (PMDTA = *N,N,N',N',N''*-penta-methyldiethylenetriamine). These species have mainly been utilised not as ligands but as precursors to phosphorus heterocycles *via* metathesis reactions with main group halides. The compound 1,2-(PhPLi)₂C₆H₄ has also been used to synthesize dichalcogenophosphinate derivatives by reaction with selenium or tellurium.⁸

The coordination chemistry of phosphido ligands is vastly different from that of neutral phosphines, which only have one lone pair and are typically π -accepting. Phosphido centres feature two lone pairs, and hence have a propensity for π -donation, making them suitable for coordination to electron-

^aDepartment of Chemistry, The University of Winnipeg, 515 Portage Avenue, Winnipeg, MB R3B 2E9, Canada^bDepartment of Chemistry and Biochemistry, University of Lethbridge, 4401 University Drive, Lethbridge, AB T1K 3M4, Canada. E-mail: p.hayes@uleth.ca; Fax: +1-403-329-2057; Tel: +1-403-329-2313

†CCDC 948785–948789. For crystallographic data in CIF or other electronic format see DOI: 10.1039/c3dt51844b

deficient early transition metals and prone to bridging bonding motifs. Accordingly, the few reports of the coordination chemistry of multidentate phosphido ligands feature mainly zirconium(IV) coordination compounds.⁹ Early examples include the zirconocene derivatives $[C\{(CH_2PPh)_2ZrCp_2\}_2]^{10}$ and $[1,2-(PPh)_2C_6H_4]ZrCp_2$.¹¹

Pincer systems featuring a single phosphido donor have recently been developed and exhibit a variety of coordination modes as well as catalytic applications. The protio PPP pincer ligand $(2-^iPr_2P-C_6H_4)_2PH$, prepared by Peters and coworkers, coordinated to copper(I) to form a binuclear complex.¹² Since this report in 2005, a number of studies involving ligands of the type $[(2-R_2P-C_6H_4)_2P]^-$ ($R = ^iPr, Ph$) have been conducted. Coordination to palladium(II) affords catalysts for the allylation of aldehydes,¹³ and organoscandium and yttrium complexes have proven useful as catalysts for the ring-opening polymerization of lactones.^{14,15} Metal complexes of platinum(II),¹⁶ rhodium(I),¹⁷ and zinc(II)¹⁸ have also been reported. Turculet *et al.* have reported the monoanionic NPN pincer ligand $[(2-Me_2N-C_6H_4)_2P]^-$ and synthesized various complexes where the ligand exhibits κ^1 -, κ^2 -, and κ^3 -binding to palladium(II).¹⁹

Recently, the groups of Turculet and Bercaw synthesized POP and PNP diphosphido pincer complexes **A**²⁰ and **B**,²¹ respectively (Chart 1). The phosphorus centres in the solid-state structures of these compounds were found to exhibit trigonal pyramidal geometry. This fact, combined with long Zr–P lengths, indicated no significant π interactions existed between the metal and P atoms of either diphosphido ligand. However, the availability of lone pairs on phosphorus for bridging multiple metals was observed in the reaction of complex **A** with either one-half or one equiv. of $[(COD)RhCl]_2$, resulting in the formation of heterobimetallic compounds with binuclear or trinuclear arrangements, respectively.¹⁵

Diphosphido pincer ligands remain exceedingly rare; in fact, the two ligands in complexes **A** and **B** are the only reported examples of such species. Hence, there is much potential for novel discoveries in the chemistry of this unique class of ancillary ligand. Accordingly, we noted that no PCP diphosphido ligands have been coordinated to metals, and that these systems might provide access to tridentate trianionic complexes *via* metallation of an aromatic C–H bond. Similar chemistry has been exploited in the synthesis of the NCN trianionic pincer complex $[2,6-(DippNCH_2)_2C_6H_2]Li_3$ (Dipp = 2,6-diisopropylphenyl).²² Given the dearth of diphosphido ligands, as well as the recent literature precedent for their preparation, we sought to generate a series of new secondary

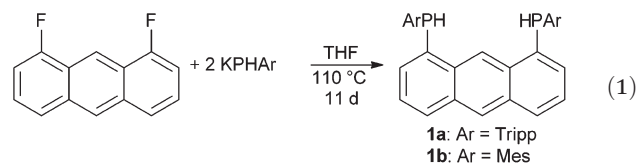
diphosphines with aromatic spacers. Herein, we report the synthesis and characterisation of two new secondary diphosphines, based on 1,8-anthracene and *m*-xylylene organic spacers, and their metallation with group 1 organometallic reagents to afford alkali metal diphosphido salts.

Results and discussion

Synthesis of diphosphines

Our initial synthetic targets, secondary diphosphines that feature aromatic frameworks, are analogues of existing tertiary phosphine-substituted compounds. Accordingly, this allowed us to capitalise upon previously established synthetic methodologies. In addition to the aforementioned applications of *m*-xylylene-bridged PCP pincer ligands, those featuring the 1,8-anthracene spacer have also been utilised for a number of purposes. For instance, the $[1,8-(^iPr_2P)_2C_{14}H_7]^-$ ligand is found in iridium(I) and (III) complexes capable of the double C–H activation of methyl *tert*-butyl ether²³ and the catalytic disproportionation of 1-hexene into hexane and 2,4-hexadiene,²⁴ respectively. We therefore pursued secondary diphosphines containing these aromatic spacers, with the long-term goal of generating transition metal diphosphido PCP complexes that might exhibit new and exciting chemical behaviour.

The starting point for the synthesis of the diphosphines 1,8-(ArPH)₂C₁₄H₈ (**1a**: Ar = Tripp; **1b**: Ar = Mes) was the preparation of 1,8-difluoroanthracene, which is a two-step procedure starting from commercially available 1,8-dichloroanthraquinone.²⁵ Once this material was prepared, the ligand synthesis was achieved by the nucleophilic aromatic substitution of 1,8-difluoroanthracene with two equiv. of KPHAr (eqn (1)), in an analogous method to the preparation of 1,8-(Ph₂P)₂C₁₄H₈,²⁵ and also similar to the route employed by Bercaw and colleagues in the synthesis of the PNP pincer ligand featured in complex **B**.²¹ Notably, this reaction employed harsh conditions, requiring heating for 6–11 d at >100 °C. While the yield was low for **1b** (20% after chromatographic purification), pure product was isolated in excellent yield for **1a** (91%).



The preparation of the *m*-xylylene-bridged ligand 1,3-(^tBuPHCH₂)₂C₆H₄ (**2**) started from α,α' -dichloro-*m*-xylene. The corresponding Grignard reagent $[1,3-(ClMgCH_2)_2C_6H_4]_x$ was formed by reaction with two equiv. of magnesium, and subsequently quenched with 2 equiv. of ^tBuPCl₂ to form the intermediary species 1,3-(^tBuPCH₂)₂C₆H₄. This compound was reduced *in situ* with LiAlH₄ to yield the desired secondary diphosphine (Scheme 1). Analysis of the dichloride (obtained directly from the reaction mixture) and crude **2** by ³¹P{¹H} NMR spectroscopy revealed that both species exist as *ca.* 1 : 1 mixtures of *rac*- and *meso*-diastereomers. Upon vacuum distillation of

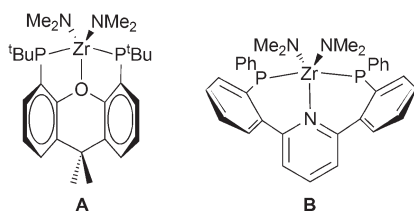
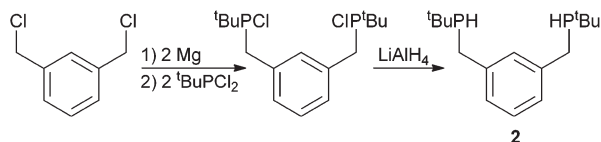
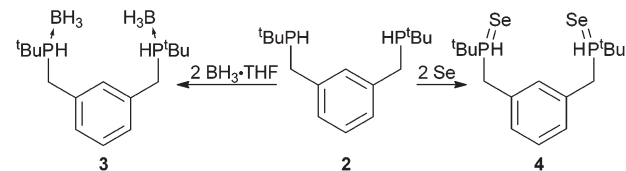


Chart 1



Scheme 1 Synthesis of diphosphine 2.



Scheme 2 Derivatisation reactions of diphosphine 2.

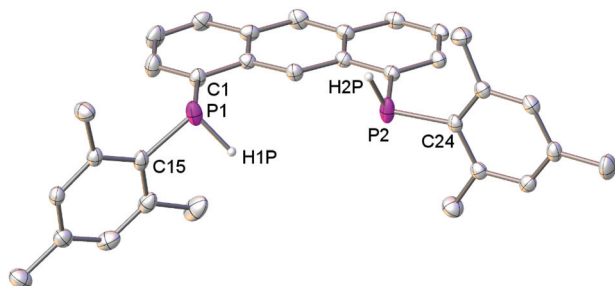


Fig. 1 Thermal ellipsoid plot (30% probability) of compound *rac*-1b. Carbon-bound hydrogen atoms are omitted for clarity. Selected bond lengths (Å) and angles (°): P1–C1 1.837(2), P1–C15 1.839(2), P2–C9 1.831(2), P2–C24 1.826(2), C1–P1–C15 103.1(1), C9–P2–C24 104.7(1).

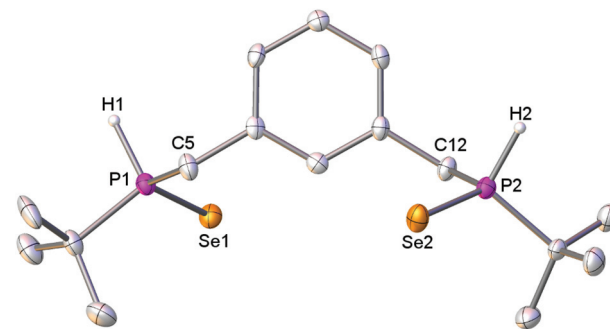


Fig. 2 Thermal ellipsoid plot (30% probability) of compound *rac*-4. Carbon-bound hydrogen atoms are omitted for clarity. Selected bond lengths (Å) and angles (°): P1–Se1 2.119(1), P1–C5 1.831(3), P2–Se2 2.110(1), P2–C12 1.823(3), C5–P1–Se1 116.2(1), C12–P2–Se2 115.7(1).

crude **2**, both diastereomers of the compound were obtained as a colourless oil that crystallized upon storage at $-35\text{ }^{\circ}\text{C}$.

Compounds **1a–b** and **2** were both fully characterised by multinuclear (^1H , $^{13}\text{C}\{^1\text{H}\}$, $^{31}\text{P}\{^1\text{H}\}$) NMR spectroscopy. The spectra were consistent with the expected solution-state structures. Notably, the presence of two diastereomers of **1a** and **1b** in *ca.* 1 : 1 ratios was evidenced by two P–H resonances in the ^1H spectra [δ 5.86, 5.81 (**1a**); 5.90, 5.88 (**1b**)], as well as two signals in the $^{31}\text{P}\{^1\text{H}\}$ spectra at δ -92.2 and -92.3 (**1a**) and -84.6 and -85.1 (**1b**). By contrast, the presence of both diastereomers of compound **2** was only evident in the $^{31}\text{P}\{^1\text{H}\}$ NMR spectrum (162.06 MHz) *via* the presence of two closely-spaced singlets at *ca.* δ -16 (3.2 Hz separation). The P–H proton resonates at δ 3.22 in the ^1H NMR spectrum. The ^{31}P chemical shifts of **1a–b** are substantially upfield from that of **2**; however, they are typical for a sterically encumbered secondary phosphine (*e.g.* δ -91.3 for Mes_2PH).²⁶ The $^1J_{\text{PH}}$ spin–spin coupling constants for **1a–b** (ranging from 220.9–223.4 Hz) and **2** (193.8 Hz) are also as expected for a secondary phosphine (*e.g.* $^1J_{\text{PH}}(\text{Ph}_2\text{PH}) = 215.6$ Hz).²⁷

We were unable to obtain X-ray quality single crystals of diphosphine **1a**, however crystals of **1b** proved suitable for structural analysis. An ellipsoid plot of the racemic isomer of **1b** is depicted in Fig. 1. Though the proposed connectivity of this mesityl derivative was unambiguously confirmed, the majority of the metrical parameters for this species are unexceptional. The two P–H functionalities are situated *anti* to each other, and the sterically demanding mesityl groups are twisted out-of-plane from the anthracene backbone at dihedral angles of 83.69(5) and 89.64(5) $^{\circ}$.

Derivatisation

Since repeated attempts to obtain X-ray quality single crystals of diphosphine **2** were unsuccessful, we focused efforts on

preparing more crystalline derivatives of this compound. The reaction of **2** with two equiv. of either $\text{BH}_3\cdot\text{THF}$ or elemental Se resulted in clean formation of diborane adduct **3** and diselenide **4**, respectively (Scheme 2), in moderate (24–65%) yields. Notably, both of these species possess diastereomers with more disparate NMR chemical shifts than those observed for the parent diphosphine **2**, and under our purification conditions each compound preferentially crystallized as a racemic mixture of one diastereomer (either *RR/SS* or *RS/SR*). Though the diborane adduct **3** tended to give thin needles upon recrystallization, crystals of **4**·2(solvent) of suitable quality and size for X-ray diffraction studies were readily obtained from a diethyl ether solution layered with pentane. A thermal ellipsoid plot of compound **4** is depicted in Fig. 2.

The particular crystal analyzed existed as a racemic mixture of (*R,R*) and (*S,S*) stereoisomers (*rac*-**4**) in the centrosymmetric space group $P2_1/c$. The metrical parameters of *rac*-**4** are consistent with typical phosphine selenides. Specifically, the P=Se distances of 2.119(1) Å and 2.110(1) Å are slightly different, though both are close to bond lengths in related compounds (*e.g.* for $\text{Ph}_2\text{P}(\text{H})\text{Se}$, $d(\text{PSe}) = 2.1109(9)$ – $2.1127(9)$ Å).²⁸

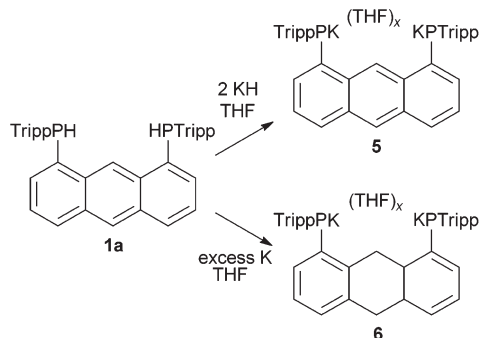
The multinuclear NMR data for compounds **3** and **4** are consistent with their formulations. The ^{31}P chemical shifts are significantly deshielded compared to the value of δ -16.1 for compound **2** (δ (**3**) 30.5; δ (**4**) 43.9), and the effect is more pronounced for **4** than **3**. Both the ^1H chemical shift (δ (**3**) 4.12; δ (**4**) 5.82) and $^1J_{\text{PH}}$ value (**3**: 362 Hz; **4**: 427 Hz) for the P–H hydrogen atom resonance also change in a similar manner. These data are consistent with the lowering of electron density at the phosphorus centres in both **3** and **4** upon coordination to a Lewis acid and oxidation, respectively.

Metalation studies

With the diphosphines **1a–b** and **2** in hand, we pursued the formation of early transition metal diphosphido complexes. Surprisingly, these species are unreactive towards both $\text{Zr}(\text{NMe}_2)_4$ and $\text{Zr}(\text{CH}_2\text{Ph})_4$, yielding no measurable reactions in C_6D_6 even at elevated temperatures for prolonged periods (100 °C, several days). By contrast, complex **B** is formed quantitatively in five minutes in an analogous fashion at ambient temperature. In the case of **1a–b**, it is possible that the bulky aromatic substituents on phosphorus prevent metallation, while for **2** the proton on the more electron-rich alkyl-substituted diphosphine is expected to be inherently less acidic. Notably, complex **A**, which features *tert*-butyl groups on phosphorus, is formed by the reaction of a dipotassium salt of the ligand, rather than amine elimination from $\text{Zr}(\text{NMe}_2)_4$.

The results of these experiments motivated us to pursue reactions with more reactive group 1 reagents. We found that the reaction of **1a** with 2 equiv. of KH in THF solution formed the dipotassium salt $1,8\text{-(TrippPK)}_2\text{C}_{14}\text{H}_8 \cdot x\text{THF}$ (**5**), which was isolated as a dark green powder in 92% yield. Interestingly, upon using an excess of potassium metal, **1a** was converted to a different dipotassium salt, $1,8\text{-(TrippPK)}_2\text{C}_{14}\text{H}_{10} \cdot x\text{THF}$ (**6**) in 89% yield (Scheme 3). In complex **6**, the anthracene framework has been formally reduced to a 9,10-dihydroanthracene, having presumably abstracted hydrogen atoms from the THF reaction solvent. Multinuclear NMR data supported the formulations of both of these species, *via* the absence of P–H resonances in the ^1H spectra, as well as significant downfield shifts in the $^{31}\text{P}\{^1\text{H}\}$ resonances ($\delta(5) -66.1$, $\delta(6) -67.8$), when compared to the value of *ca.* $\delta -92$ observed for **1a**.

Although X-ray quality single crystals of compounds **5** and **6** were not obtained in our hands, reaction of **6** with H_2O followed by crystallization of the major hydrolysis product from benzene resulted in crystals of the protio derivative $(\text{TrippPH})_2\text{C}_{14}\text{H}_{10} \cdot 0.5(\text{C}_6\text{H}_6)$,²⁹ as determined by XRD studies. Additionally, the crown ether derivative of **6**, $[\text{K}(18\text{-crown-6})(\text{THF})_2]_2[1,8\text{-(TrippP)}_2\text{C}_{14}\text{H}_{10}]$ (**7**) also proved suitable for solid-state characterisation. Thermal ellipsoid plots of $(\text{TrippPH})_2\text{C}_{14}\text{H}_{10}$ and the dianion of **7** are depicted in Fig. 3 and 4, respectively. These crystal structures served as confirmations of the expected structures; notably, the C–P–C bond angles did not change significantly upon removal of the P–H protons.



Scheme 3 Formation of dipotassium salts **5** and **6**.

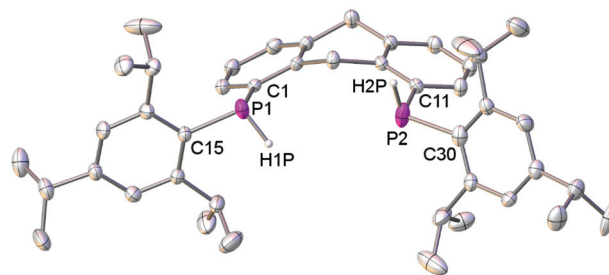


Fig. 3 Thermal ellipsoid plot (30% probability) of $(\text{TrippPH})_2\text{C}_{14}\text{H}_{10}$. The solvent of crystallization (C_6H_6) and carbon-bound hydrogen atoms are removed for clarity. Selected bond lengths (Å) and angles (°): P1–C1 1.835(3), P1–C15 1.832(2), P2–C11 1.823(3), P2–C30 1.866(3), C1–P1–C15 103.8(1), C11–P2–C30 103.2(2).

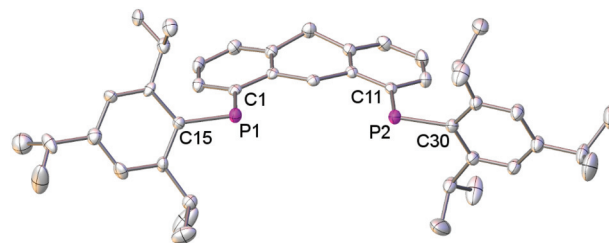
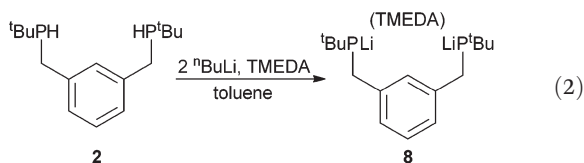


Fig. 4 Thermal ellipsoid plot (30% probability) of the dianion of complex **7**. Two $[\text{K}(18\text{-crown-6})(\text{THF})_2]^+$ cations and hydrogen atoms have been removed for clarity. Selected bond lengths (Å) and angles (°): P1–C1 1.797(3), P1–C15 1.875(11), P2–C11 1.795(3), P2–C30 1.877(3), C1–P1–C15 102.2(3), C11–P2–C30 102.2(2).

Diphosphine **2** was also subjected to metallation studies. A solution of **2** in toluene was found to react with 2 equiv. each of $^n\text{BuLi}$ and TMEDA to form the coordination compound $1,3\text{-}(^n\text{BuPLiCH}_2)_2\text{C}_6\text{H}_4 \cdot \text{TMEDA}$ (**8**) as an analytically pure yellow powder in high (89%) yield (eqn (2)). Whereas **5–7** are essentially insoluble in most organic solvents except for THF, **8** exhibits substantial solubility in benzene, and is even sparingly soluble in pentane. Although variable temperature NMR spectra of **8** generally featured broad resonances with no discernable spin–spin coupling, the ^1H NMR spectrum revealed the expected lack of P–H resonances. Interestingly, ^1H integrations revealed that only one molecule of TMEDA was present per diphosphido ligand, though enough was present in the reaction mixture to afford a 2 : 1 ratio. The $^{31}\text{P}\{^1\text{H}\}$ NMR spectrum exhibited a single broad resonance at $\delta -0.5$, a significant downfield shift from the parent compound **2**. X-ray quality single crystals of **8** were grown from a pentane solution, allowing for elucidation of its solid-state structure; a thermal ellipsoid plot is depicted in Fig. 5.



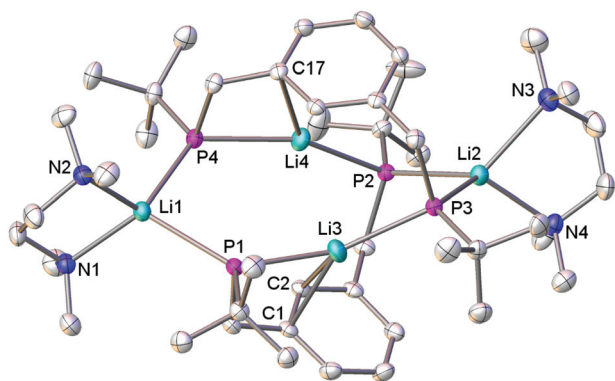


Fig. 5 Thermal ellipsoid plot (30% probability) of complex **8**. Hydrogen atoms are omitted for clarity. Selected bond lengths (Å) and angles (°): N1–Li1 2.212(4), N2–Li1 2.160(4), N3–Li2 2.337(4), N4–Li2 2.192(4), P1–Li1 2.583(4), P1–Li3 2.480(4), P2–Li2 2.634(4), P2–Li4 2.486(4), P3–Li2 2.635(3), P3–Li3 2.451(4), P4–Li1 2.599(4), P4–Li4 2.495(4), Li3–C1 2.533(5), Li3–C2 2.683(5), Li4–C17 2.557(4), Li1–P1–Li3 127.9(1), Li2–P2–Li4 109.0(1), Li2–P3–Li3 110.9(1), Li1–P4–Li4 126.3(1).

The solid-state structure of complex **8** revealed a dimeric arrangement featuring an eight-membered Li_4P_4 ring with $d(\text{Li}–\text{P}) = 2.451(4)–2.635(3)$ Å. The bonding motif of a Li_4P_4 ring has been previously observed in the crystal structures of a variety of main group compounds, such as the species $\{[\text{Li}(\text{THF})_2][\text{PhPCH}_2\text{CH}_2\text{PPh}]_2\}$,⁵ which features similar lithium–phosphorus bond distances of 2.57(1) Å and 2.57(2) Å. In this diphosphido analogue of 1,2-bis(diphenylphosphino)ethane, two lithium ions are *P,P*-chelated to one ligand, and two are *P,P*-bridged across both ligands; each lithium ion is also coordinated to two THF molecules. By contrast, in compound **8** two of the lithium ions are four-coordinate, bound by a single TMEDA donor as well as two phosphides, while the remaining two are each coordinated to two phosphides as well as an aromatic ring of one of the ligands *via* weak secondary bonding interactions. All four lithium ions in **8** are bridged between the two diphosphido ligands. The closest $\text{Li}\cdots\text{C}$ contacts, from Li3 to the nearest aromatic *ipso*-carbon atom, and from Li4 to the nearest aromatic *ipso*- and *ortho*-carbon atoms, have distances in the range of 2.533(5)–2.683(5) Å, which are well below the sum of the van der Waals radii of these atoms.³⁰ The carbon atoms involved in these contacts are not significantly distorted from planarity; the sums of the bond angles are *ca.* 360°, except for the angles about C2 which add to *ca.* 357°. The $\text{Li}\cdots\text{C}$ distances are longer than the averages observed in other structures featuring electrostatic lithium \cdots carbon interactions, *e.g.* 2.33 Å in $[\text{Li}(\text{Et}_2\text{O})_4][\text{Zr}(\text{biphe})_4]$ (biphe = 2,2'-biphenyl-diyl)³¹ and 2.42 Å in $[\text{Li}(\text{TMEDA})_2][\text{C}_{10}\text{H}_8]$.³²

It is unknown if the dimeric arrangement persists in solution, though the NMR data are consistent with a similar structure in which both halves of the dimer are chemically equivalent on the NMR timescale. The formation of a dimer instead of a monomeric species seems to indicate the predilection for the phosphido functionalities to bridge two metal centres.

Attempted metathesis chemistry

Given the lack of reactivity of compounds **1a–b** and **2** with transition metal alkyl and amide reagents, we pursued the reaction of alkali metal derivatives **5** and **8** with various transition metal halides. Some of the compounds tested were $[\text{IrCl}_3(\text{MeCN})_3]$, $[(\text{COD})\text{PtCl}_2]$ (COD = 1,5-cyclooctadiene), $[(\eta^5\text{-C}_5\text{H}_5)_2\text{TiCl}_2]$, Me_3TaCl_2 and $\text{NiCl}_2(\text{dme})$ (dme = 1,2-dimethoxyethane). Unfortunately, in all cases either no reaction occurred, or intractable mixtures were obtained which often featured the protio ligands **1a** or **2** as components. This indicated the possibility that undesirable redox chemistry was occurring in solution, resulting in hydrogen atom abstraction from the reaction solvent.

In an attempt to tame the undesired reactivity of the dianionic phosphido ligand, a borane-protected analogue was prepared for use in metathetical reactions. Relatedly, the protected diphosphido species $[\text{PhP}(\text{BH}_3)\text{CH}_2\text{CH}_2\text{P}(\text{BH}_3)\text{Ph}]^{2-}$ was observed to act as a bridging ligand towards two $[(\eta^5\text{-C}_5\text{H}_5)\text{Fe}(\text{CO})_2]^+$ fragments, as reported by Wagner and coworkers in 2007.³³

The addition of two equiv. of *n*-BuLi to a THF solution of the borane derivative **3** at -78 °C resulted in formation of a new species with no P–H groups, as determined by *in situ* ^{31}P NMR spectroscopy ($\delta -16.2$) and consistent with the desired borane-protected dilithio compound. A small amount of the putative monolithio species was also observed as two ^{31}P resonances (δ 31.2, -13.9); the downfield signal exhibited P–H coupling consistent with a one-bond interaction (*ca.* 350 Hz).

The reaction of aliquots of this solution with various transition metal halide salts were conducted (including $\text{NiCl}_2(\text{dme})$, ZnCl_2 , TaCl_5 , and $\text{ZrCl}_4(\text{THF})_2$) and monitored by *in situ* ^{31}P NMR spectroscopy. Once again, no clean reactivity was observed, and all the resultant mixtures featured large amounts and numbers of P–H-containing species.

Experimental

General experimental procedures

All manipulations were performed under an atmosphere of argon using standard glovebox or vacuum line techniques. The solvents diethyl ether, tetrahydrofuran (THF), pentane, benzene, toluene and dichloromethane were purified by sparging with argon gas followed by passage through two alumina columns, and were freshly distilled from sodium benzophenone ketyl (THF and diethyl ether), “titanocene” indicator (toluene, benzene and pentane) or calcium hydride (CH_2Cl_2) when needed. Deuterated solvents were dried over sodium benzophenone ketyl (*d*₈-THF and C_6D_6) or calcium hydride (CDCl_3 , *d*₆-DMSO and CD_2Cl_2), degassed using at least three freeze–pump–thaw cycles and distilled into PTFE-sealed flasks containing activated 4 Å molecular sieves. NMR spectra were recorded at ambient temperature on either a 300 MHz Bruker Avance II (Ultraschield) spectrometer (^1H : 300.13 MHz, $^{13}\text{C}\{^1\text{H}\}$: 75.47 MHz, $^{31}\text{P}\{^1\text{H}\}$: 121.49 MHz) or a 400 MHz Bruker Avance III (Ultraschield) spectrometer (^1H : 400.33 MHz, $^{13}\text{C}\{^1\text{H}\}$:

100.66 MHz, $^{31}\text{P}\{^1\text{H}\}$: 162.06 MHz, $^{11}\text{B}\{^1\text{H}\}$: 128.44 MHz, $^{77}\text{Se}\{^1\text{H}\}$: 76.35 MHz). NMR resonances are reported in parts per million (ppm) and referenced relative to SiMe_4 (^1H and $^{13}\text{C}\{^1\text{H}\}$, δ 0) *via* residual ^1H or ^{13}C resonances of the deuterated solvent, or to the external references 85% $\text{H}_3\text{PO}_4(\text{aq.})$ ($^{31}\text{P}\{^1\text{H}\}$, δ 0), neat $\text{BF}_3\cdot\text{Et}_2\text{O}$ ($^{11}\text{B}\{^1\text{H}\}$, δ 0), or 1 M Ph_2Se_2 in CDCl_3 ($^{77}\text{Se}\{^1\text{H}\}$, δ 463). ^{13}C assignments were aided by the use of additional experiments, such as HSQC, APT and ^1H -coupled ^{13}C NMR spectra. Elemental analyses were conducted using an Elementar Americas Vario Microcube instrument. The reagents 1,8-difluoroanthracene²⁵ and KPHAr (Ar = Tripp, Mes)³⁴ were prepared using modifications of the literature procedures. TMEDA was dried over CaH_2 and distilled into a PTFE-sealed bomb containing activated 4 Å molecular sieves. All other reagents were purchased from commercial sources and used as received.

Synthesis and characterisation

Preparation of 1,8-(TrippPH) $_2\text{C}_{14}\text{H}_8$ (1a). A 250 mL PTFE-sealed bomb was charged with 1,8-difluoroanthracene (1.22 g, 5.68 mmol) and KPHTripp (3.28 g, 11.9 mmol). THF (120 mL) was transferred to the reaction vessel, resulting in a colour change of the mixture from yellow to dark green. The resulting solution was heated to 110 °C for 11 d. After cooling to ambient temperature, the volatiles were removed under vacuum and CH_2Cl_2 (90 mL) was added by vacuum transfer. The resulting green solution was filtered through silica gel with a swivel frit apparatus attached to a 2-neck, 250 mL round-bottom flask. The red filtrate was then concentrated under vacuum affording *rac/meso*-1a as a yellow-orange solid (3.33 g, 91%, m.p. 87–88 °C). ^1H NMR (CDCl_3): δ 9.32 (s, 1H, anthracene 9-*H*), 8.50 (s, 1H, anthracene 10-*H*), 7.93 (d, 2H, $^3J_{\text{HH}} = 8.7$ Hz, anthracene 4,5-*H*), 7.37–7.24 (m, 2H, anthracene 3,6-*H*), 7.21 (s, 4H, Tripp aromatic 3,5-*H*), 7.06–6.91 (m, 2H, anthracene 2,7-*H*), 5.86 (d, 1H, $^1J_{\text{HP}} = 223.3$ Hz, PH), 5.81 (d, 1H, $^1J_{\text{HP}} = 220.9$ Hz, PH), 3.75–3.56 (m, 4H, Tripp 2,6- $\text{CH}(\text{CH}_3)_2$), 3.01 (sp, 2H, $^3J_{\text{HH}} = 6.9$ Hz, Tripp 4- $\text{CH}(\text{CH}_3)_2$), 1.37 (d, 12H, $^3J_{\text{HH}} = 6.9$ Hz, Tripp 4- $\text{CH}(\text{CH}_3)_2$), 1.31–1.07 (m, 24H, Tripp 2,6- $\text{CH}(\text{CH}_3)_2$). $^{13}\text{C}\{^1\text{H}\}$ NMR (CDCl_3): δ 154.9 (d, $^2J_{\text{CP}} = 12.6$ Hz, Tripp aromatic 2,6-*C*), 150.9 (s, Tripp aromatic 4-*C*), 134.6 (d, $^2J_{\text{CP}} = 18.6$ Hz, anthracene 1a,8a-*C*), 132.4 (d, $^1J_{\text{CP}} = 15.8$ Hz, Tripp aromatic 1-*C*), 131.5 (d, $^3J_{\text{CP}} = 2.2$ Hz, anthracene 4a,5a-*C*), 130.0 (br s, anthracene 2,7-*C*), 128.2 (s, anthracene 10-*C*), 128.1 (s, anthracene 4,5-*C*), 125.4 (s, anthracene 3,6-*C*), 124.8 (d, $^1J_{\text{CP}} = 9.5$ Hz, anthracene 1,8-*C*), 122.0 (d, $^3J_{\text{CP}} = 3.9$ Hz, Tripp 3,5-*C*), 121.2 (t, $^3J_{\text{CP}} = 20.9$ Hz, anthracene 9-*C*), 34.5 (s, Tripp 4- $\text{CH}(\text{CH}_3)_2$), 33.1 (d, $^3J_{\text{CP}} = 14.3$ Hz, Tripp 2,6- $\text{CH}(\text{CH}_3)_2$), 25.2 (s, Tripp 2,6- $\text{CH}(\text{CH}_3)_2$), 24.4 (s, Tripp 2,6- $\text{CH}(\text{CH}_3)_2$), 24.1 (s, Tripp 4- $\text{CH}(\text{CH}_3)_2$). ^{31}P NMR (CDCl_3): δ -92.2 (d, $^1J_{\text{PH}} = 223.3$ Hz), -92.3 (d, $^1J_{\text{PH}} = 220.9$ Hz). Anal. Calcd (%) for $\text{C}_{44}\text{H}_{56}\text{P}_2$: C: 81.70; H: 8.73; found: C: 81.70; H: 8.70.

Preparation of 1,8-(MesPH) $_2\text{C}_{14}\text{H}_8$ (1b). A 100 mL PTFE-sealed bomb was charged with 1,8-difluoroanthracene (0.51 g, 2.39 mmol) and KPHMes (0.96 g, 5.03 mmol). THF (55 mL) was transferred to the reaction vessel, and the resulting

solution was heated to 130 °C for 6 d. After cooling to ambient temperature, the volatiles were removed under vacuum, affording a brown solid. This was dissolved in CH_2Cl_2 (50 mL) and the resulting solution was filtered through silica gel with a swivel frit apparatus attached to a 2-neck, 100 mL round-bottom flask. The silica gel was washed with 95 : 5 hexanes-dichloromethane (4 × 25 mL), and the combined organic filtrate was then concentrated under vacuum affording crude **1b** as an orange solid. The compound was purified by flash column chromatography, eluting with 9 : 1 toluene–heptane and under an atmosphere of argon, yielding pure *rac/meso*-1b as a yellow solid (0.11 g, 20%, m.p. 87–88 °C). ^1H NMR (C_6D_6): δ 9.67 (s, 0.5H, anthracene 9-*H*), 9.55 (s, 0.5H, anthracene 9-*H*), 8.16 and 8.14 (overlapping s, 1H, anthracene 10-*H*), 7.68 (d, 2H, $^3J_{\text{HH}} = 8.5$ Hz, anthracene 4,5-*H*), 7.30 (ov dd, 1H, $^3J_{\text{HH}} = 6.7$ Hz, $^3J_{\text{PH}} = 6.9$ Hz, anthracene 2,7-*H*), 7.17 (br ov m, anthracene 2,7-*H* overlapping with $\text{C}_6\text{D}_5\text{H}$ resonance), 7.02–6.99 (m, 2H, anthracene 3,6-*H*), 6.84 and 6.82 (overlapping s, 4H, Mes aromatic 3,5-*H*), 5.90 and 5.88 (ov d, 2H, $^1J_{\text{PH}} = 223.4$ Hz, PH), 2.40 and 2.38 (ov s, 12H, Mes 2,6- CH_3), 2.14 and 2.13 (ov s, 6H, Mes 4- CH_3). $^{13}\text{C}\{^1\text{H}\}$ NMR (CDCl_3): δ 144.0 (d, $J_{\text{PC}} = 13.3$ Hz), 143.4 (d, $J_{\text{PC}} = 12.9$ Hz), 139.3 (s), 138.9 (s), 132.7 (ov m), 132.6 (ov m), 131.44 (s), 130.5 (s), 130.41 (s), 130.3 (s), 129.3 (s), 129.2 (s), 128.6 (br s), 128.2 (br s), 127.7 (d, $J_{\text{PC}} = 10.9$ Hz), 127.2 (d, $J_{\text{PC}} = 10.2$ Hz), 125.4 (br s), 122.3 (t, $J_{\text{PC}} = 16.9$ Hz), 121.8 (t, $J_{\text{PC}} = 19.5$ Hz), 23.3 (s), 23.1 (s), 21.2 (s), 21.1 (s). $^{31}\text{P}\{^1\text{H}\}$ NMR (C_6D_6): δ -84.6 (s), -85.1 (s). ^{31}P NMR (C_6D_6): δ -84.6 (br d, $^1J_{\text{PH}} = 223.8$ Hz), -85.1 (br d, $^1J_{\text{PH}} = 221.4$ Hz). Anal. Calcd (%) for $\text{C}_{32}\text{H}_{32}\text{P}_2$: C: 80.31; H: 6.74; found: C: 80.50; H: 7.45.

Preparation of 1,3-($^t\text{BuPHCH}_2$) $_2\text{C}_6\text{H}_4$ (2). THF (100 mL) was added to a flask containing α,α' -dichloro-*m*-xylene (5.00 g, 28.6 mmol) and magnesium turnings (1.40 g, 57.6 mmol). The resulting mixture was stirred at ambient temperature for 5 h, then at 40 °C for 17 h. The dark yellow solution was cooled to -78 °C and added to a solution of *tert*-butyldichlorophosphine (9.21 g, 57.9 mmol) in THF (150 mL) at -78 °C dropwise, *via* a cannula. After warming to ambient temperature, the resulting mixture was stirred for 1 h, then cooled to 0 °C. A suspension of LiAlH_4 (840 mg, 22.1 mmol) in THF (25 mL) at 0 °C was added to the mixture, which was allowed to warm to ambient temperature and then stirred for 18 h. The volatiles were then removed under vacuum, yielding a sticky grey mass which was extracted with heptane (4 × 25 mL). The combined washings were filtered through a coarse porosity fritted funnel, and the volatiles were removed under vacuum to yield an opaque grey oil. Purification was performed by distilling the crude product twice under dynamic vacuum, yielding pure **2** as a colourless oil (2.12 g, 26%), which crystallized upon storage at -35 °C. ^1H NMR (C_6D_6): δ 7.24 (s, 1H, aromatic 2-*H*), 7.14–7.06 (m, 1H, aromatic 5-*H*), 7.05–7.00 (m, 2H, aromatic 4,6-*H*), 3.22 (ddd, 2H, $^1J_{\text{HP}} = 193.8$ Hz, $^3J_{\text{HH}} = 10.2$ Hz, 5.5 Hz, P-*H*), 3.04–2.96 (m, 2H, CH_2), 2.66–2.55 (m, 2H, CH_2), 1.06 (d, 18H, $^3J_{\text{HP}} = 11.5$ Hz, $\text{C}(\text{CH}_3)_3$). $^{13}\text{C}\{^1\text{H}\}$ NMR (C_6D_6): 140.6 (d, $^2J_{\text{CP}} = 5.4$ Hz, aromatic 1,3-*C*), 130.2 (t, $^3J_{\text{CP}} = 5.9$ Hz, aromatic 2-*C*), 129.3 (s, aromatic 5-*C*), 127.0 (d, $^3J_{\text{CP}} = 5.5$ Hz, aromatic 4,6-*C*), 30.4 (d, $^2J_{\text{CP}} = 12.6$ Hz,

$C(CH_3)_3$, 27.8 (d, $^1J_{CP} = 10.7$ Hz, $C(CH_3)_3$), 26.1 (d, $^1J_{CP} = 18.3$ Hz, CH_2P). $^{31}P\{^1H\}$ NMR (C_6D_6 , 162.06 MHz): δ -16.19 (s), -16.21 (s). ^{31}P NMR (C_6D_6): δ -16.1 (br d, $^1J_{PH} = 193.8$ Hz). Anal. Calcd (%) for $C_{16}H_{28}P_2$: C: 68.06; H: 10.00; found: C: 67.91; H: 9.92.

Preparation of 1,3-(t -BuPH(BH $_3$)CH $_2$) $_2$ C $_6$ H $_4$ (3). BH $_3$ ·THF (1.42 mL, 1.0 M in THF, 1.42 mmol) was added to a solution of **2** (197 mg, 0.70 mmol) in Et $_2$ O (20 mL), and the resulting clear colourless solution was stirred at ambient temperature for 2 h. Removal of the volatiles under vacuum yielded an oil, which was dissolved in toluene and stored at -35 °C. Crystallization occurred after several days; the toluene was decanted, and the remaining material dried under vacuum to afford colourless crystals of analytically pure **3** (52 mg, 24%, m.p. 102–105 °C). 1H NMR (C_6D_6): δ 7.15–7.05 (br m, 1H, aromatic 5-*H*), 7.01–6.93 (br m, 2H, aromatic 4,6-*H*), 4.12 (br dm, 2H, $^1J_{HP} = 362.0$ Hz, *P-H*), 2.87–2.71 (m, 2H, CH_2), 2.71–2.55 (m, 2H, CH_2), 1.30 (br m, overlapping with $C(CH_3)_3$ signal, 6H, BH $_3$), 0.94 (d, 18H, $^3J_{HP} = 14.2$ Hz, $C(CH_3)_3$). The aromatic 2-*H* resonance is obscured underneath the C_6D_5H signal. Evidence of a minor diastereomer was observed *via* a resonance overlapping with the $C(CH_3)_3$ signal. $^{11}B\{^1H\}$ NMR (C_6D_6): δ -41.96 (d, $^1J_{BP} = 38.5$ Hz). $^{13}C\{^1H\}$ NMR (C_6D_6): δ 135.5 (dd, $^2J_{CP} = 5.9$ Hz, $^4J_{CP} = 2.0$ Hz, aromatic 1,3-*C*), 131.6 (t, $^3J_{CP} = 4.4$ Hz, aromatic 2-*C*), 129.5 (m, aromatic 4,6-*C*), 128.5 (overlapping with C_6D_6 resonance, aromatic 5-*C*), 27.6 (d, $^1J_{CP} = 30.7$ Hz, $C(CH_3)_3$), 26.9 (m, $C(CH_3)_3$), 26.3 (d, $^1J_{CP} = 27.6$ Hz, CH_2P). Distinct resonances corresponding to a minor diastereomer were observed for the aromatic 2-*C*, $C(CH_3)_3$, and CH_2P carbon atoms. $^{31}P\{^1H\}$ NMR (C_6D_6): δ 30.5 (br s). ^{31}P NMR (C_6D_6): δ 30.5 (br d, $^1J_{PH} = 362.0$ Hz). Anal. Calcd (%) for $C_{16}H_{34}B_2P_2$: C: 61.99; H: 11.05; found: C: 61.59; H: 10.80.

Preparation of 1,3-(t -BuPH(Se)CH $_2$) $_2$ C $_6$ H $_4$ (4). Grey selenium (87.0 mg, 1.10 mmol) was added to a solution of **2** (150 mg, 0.531 mmol) in THF (20 mL). The mixture was stirred at ambient temperature for 18 h, and then the volatiles were removed under vacuum to generate a grey oil. Dissolution of the oil in a minimal amount of benzene resulted in the precipitation of crystalline material, and subsequent removal of volatiles under vacuum afforded **4** as an off-white crystalline solid (151 mg, 65%, m.p. 149–150 °C). NMR data indicated **4** was isolated as a mixture of *rac*- and *meso*-diastereomers. 1H NMR ($CDCl_3$): δ 7.35 (br s, 1H, aromatic 2-*H*), 7.30–7.33 (m, 1H, aromatic 5-*H*), 7.19–7.26 (br m, 2H, aromatic 4,6-*H*), 5.82 (ddd, 2H $^1J_{HP} = 427.0$ Hz, $^3J_{HH} = 7.4$ Hz, 1.4 Hz, *P-H*), 3.83–3.74 (m, 2H, CH_2), 3.28–3.14 (m, 2H, CH_2) 1.33 (d, 18H, $^3J_{HP} = 18.3$ Hz, $C(CH_3)_3$). Several resonances for a minor diastereomer were observed, overlapping with the *P-H* and $C(CH_3)_3$ signals. $^{13}C\{^1H\}$ NMR ($CDCl_3$): δ 133.2 (m, aromatic 1,3-*C*), 131.4 (t, $^3J_{CP} = 5.3$ Hz, aromatic 2-*C*), 129.4 (t, $^4J_{CP} = 2.9$ Hz, aromatic 5-*C*), 128.7 (t, $^3J_{CP} = 4.4$ Hz, aromatic 4,6-*C*), 34.2 (d, $^1J_{CP} = 35.9$ Hz, CH_2P), 32.5 (d, $^1J_{CP} = 40.2$ Hz, $C(CH_3)_3$), 25.8 (m, $C(CH_3)_3$). $^{31}P\{^1H\}$ NMR ($CDCl_3$): δ 43.9 (s, $^1J_{PSe} = 722.8$ Hz, 83%, major diastereomer), 43.4 (d, $^1J_{PSe} = 721.6$ Hz, 17%, minor diastereomer). ^{31}P NMR ($CDCl_3$): δ 43.9 (br d, $^1J_{PH} = 427.7$ Hz). $^{77}Se\{^1H\}$ NMR ($CDCl_3$): δ -427.3 (d, $^1J_{SeP} = 722.8$ Hz).

A resonance for a minor diastereomer was observed at δ -426.8 (d, $^1J_{SeP} = 721.6$ Hz). Recrystallization from toluene afforded an analytically pure solid. Anal. Calcd (%) for $C_{16}H_{28}P_2Se_2$: C: 43.65; H: 6.41; found: C: 43.83; H: 6.33. X-ray quality single crystals of **4**·(solvent) were grown from a solution of the compound in diethyl ether layered with pentane.

Preparation of 1,8-(TrippPK) $_2$ C $_{14}$ H $_{10}$ ·*x*THF (5). A solution of **1** (586 mg, 0.906 mmol) in THF (13 mL) was added to a suspension of KH (72.7 mg, 1.81 mmol) in THF (2 mL). Within minutes of initiating the reaction, a colour change of the mixture from yellow to brown and finally to dark green was observed. The reaction mixture was stirred for 20 h at ambient temperature. After centrifugation to remove residual KH, the dark green solution was concentrated under vacuum affording **5** as a dark green powder (696 mg, 92%, m.p. 229–230 °C). The degree of THF solvation in the isolated product was calculated as $x = 1.5$ by 1H NMR spectroscopy in d_6 -DMSO. 1H NMR (d_6 -DMSO): δ 9.53 (t, 1H, $^4J_{HP} = 6.0$ Hz, anthracene 9-*H*), 7.13 (s, 1H, anthracene 10-*H*), 6.87 (s, 4H, Tripp 3,5-*H*), 6.20–6.05 (m, 4H, anthracene 3,4,5,6-*H*), 5.70 (d, 2H, $^3J_{HH} = 6.9$ Hz, anthracene 2,7-*H*), 4.49–4.26 (m, 4H, Tripp 2,6-*CH(CH_3)_2*), 3.69–3.51 (m, 6H, THF), 2.81 (sp, 2H, $^3J_{HH} = 6.9$ Hz, Tripp 4-*CH(CH_3)_2*), 1.82–1.69 (m, 6H, THF), 1.24 (d, 12H, $^3J_{HH} = 6.9$ Hz, Tripp 4-*CH(CH_3)_2*), 1.10 (d, 24H, $^3J_{HH} = 6.9$ Hz, Tripp 2,6-*CH(CH_3)_2*). 1H NMR (d_8 -THF): δ 9.76 (t, 1H, $^4J_{HP} = 7.2$ Hz, anthracene 9-*H*), 7.58 (s, 1H, anthracene 10-*H*), 6.97 (s, 4H, Tripp 3,5-*H*), 6.58 (d, 2H, $^3J_{HH} = 7.8$ Hz, anthracene 4,5-*H*), 6.50 (t, 2H, $^3J_{HH} = 7.8$ Hz, anthracene 3,6-*H*), 6.17 (d, 2H, $^3J_{HH} = 7.8$ Hz, anthracene 2,7-*H*), 4.58–4.39 (m, 4H, Tripp 2,6-*CH(CH_3)_2*), 2.86 (sp, 2H, $^3J_{HH} = 6.9$ Hz, Tripp 4-*CH(CH_3)_2*), 1.28 (d, 12H, $^3J_{HH} = 6.9$ Hz, Tripp 4-*CH(CH_3)_2*), 1.16 (d, 24H, $^3J_{HH} = 6.9$ Hz, Tripp 2,6-*CH(CH_3)_2*). $^{13}C\{^1H\}$ NMR (d_8 -THF): δ 162.0 (d, $^1J_{CP} = 55.1$ Hz, Tripp 1-*C*), 155.33 (d, $^4J_{CP} = 3.0$ Hz, Tripp 4-*C*), 155.28 (d, $^4J_{CP} = 3.8$ Hz, Tripp 4-*C*), 146.1 (s, anthracene 1a,8a-*C* or 4a,5a-*C*), 143.1 (d, $^1J_{CP} = 42.3$ Hz, anthracene 1,8-*C*), 133.8 (s, anthracene 1a,8a-*C* or 4a,5a-*C*), 131.81 (d, $^2J_{CP} = 24.9$ Hz, Tripp 2,6-*C*), 131.76 (d, $^2J_{CP} = 24.9$ Hz, Tripp 2,6-*C*), 126.0 (s, anthracene 3,6-*C*), 125.3 (s, anthracene 10-*C*), 120.8 (s, Tripp 3,5-*C*), 118.9 (s, anthracene 2,7-*C*), 118.9 (t, $^3J_{CP} = 39.2$ Hz, anthracene 9-*C*), 112.8 (d, $^4J_{CP} = 5.3$ Hz, anthracene 4,5-*C*), 68.4 (s, THF), 35.5 (s, Tripp 4-*CH(CH_3)_2*), 34.0 (d, $^3J_{CP} = 12.1$ Hz, Tripp 2,6-*CH(CH_3)_2*), 26.6 (s, THF), 26.1 (s, overlapping with d_8 -THF signal, Tripp 2,6-*CH(CH_3)_2*), 25.6 (s, overlapping with d_8 -THF signal, Tripp 2,6-*CH(CH_3)_2*), 24.9 (s, overlapping with d_8 -THF signal, Tripp 4-*CH(CH_3)_2*). $^{31}P\{^1H\}$ NMR (121.5 MHz, d_6 -DMSO): δ -35.9 (s). $^{31}P\{^1H\}$ NMR (d_8 -THF): δ -66.1 (s). Anal. Calcd (%) for $C_{44}H_{54}K_2P_2$ ·THF: C: 72.50; H: 7.86; found: C: 72.46; H: 7.97.

Preparation of 1,8-(TrippPK) $_2$ C $_{14}$ H $_{10}$ ·*x*THF (6). A flask was charged with **1** (615 mg, 0.951 mmol) and potassium (157 mg, 4.02 mmol). THF (10 mL) was transferred to the reaction vessel, resulting in a colour change of the mixture from orange to green and finally to dark brown. The ensuing solution was stirred for 20 h at ambient temperature. The mixture was transferred to a separate flask *via* a cannula to remove excess potassium. Upon removal of the volatiles under vacuum, a brown

solid was obtained. The residue was washed with cold ($-35\text{ }^{\circ}\text{C}$) pentane ($2 \times 2\text{ mL}$) and dried under reduced pressure to afford **6** as a brown powder (673 mg, 89%, m.p. $>350\text{ }^{\circ}\text{C}$). The degree of THF solvation in the isolated product was calculated as $x = 1$ by ^1H NMR spectroscopy in C_6D_6 . ^1H NMR (d_8 -THF): δ 6.92 (s, 4H, Tripp 3,5-*H*), 6.43–6.26 (m, 4H, 9,10-dihydroanthracene *CH*), 6.12–6.02 (m, 2H, 9,10-dihydroanthracene *CH*), 4.62–4.43 (m, 4H, Tripp 2,6-*CH*(CH_3)₂), 3.70 (s, 2H, overlapping with d_8 -THF signal, 9,10-dihydroanthracene 10-*CH*₂), 2.93–2.73 (m, 2H, Tripp 4-*CH*(CH_3)₂), 1.25 (d, 12H, $^3J_{\text{HH}} = 6.3\text{ Hz}$, Tripp 4-*CH*(CH_3)₂), 1.19–1.02 (m, 24H, Tripp 2,6-*CH*(CH_3)₂). The second 9,10-dihydroanthracene *CH*₂ signal was obscured by Tripp *CH*(CH_3)₂ resonances. $^{13}\text{C}\{^1\text{H}\}$ NMR (d_8 -THF): δ 161.4 (d, $^1J_{\text{CP}} = 53.6\text{ Hz}$, Tripp 1-*C*), 155.4 (d, $^4J_{\text{CP}} = 3.8\text{ Hz}$, Tripp 4-*C*), 155.3 (d, $^4J_{\text{CP}} = 3.8\text{ Hz}$, Tripp 4-*C*), 145.8 (s, 9,10-dihydroanthracene 1a,8a-*C* or 4a,5a-*C*), 144.2 (d, $^1J_{\text{CP}} = 43.0\text{ Hz}$, 9,10-dihydroanthracene 1,8-*C*), 133.5 (s, 9,10-dihydroanthracene 1a,8a-*C* or 4a,5a-*C*), 130.44 (d, $^2J_{\text{CP}} = 27.2\text{ Hz}$, Tripp 2,6-*C*), 130.39 (d, $^2J_{\text{CP}} = 27.2\text{ Hz}$, Tripp 2,6-*C*), 124.7 (s, 9,10-dihydroanthracene *CH*), 124.3 (s, 9,10-dihydroanthracene *CH*), 120.6 (s, Tripp 3,5-*C*), 114.2 (s, 9,10-dihydroanthracene *CH*), 68.4 (s, THF), 37.1 (s, 9,10-dihydroanthracene 10-*C*), 35.6 (s, Tripp 4-*CH*(CH_3)₂), 33.8 (d, $^3J_{\text{CP}} = 12.1\text{ Hz}$, Tripp 2,6-*CH*(CH_3)₂), 26.6 (s, THF), 25.8 (s, overlapping with d_8 -THF signal, Tripp 2,6-*CH*(CH_3)₂), 25.7 (s, overlapping with d_8 -THF signal, Tripp 2,6-*CH*(CH_3)₂), 25.0 (s, overlapping with d_8 -THF signal, Tripp 4-*CH*(CH_3)₂). The 9,10-dihydroanthracene 9-*C* signal was not observed. $^{31}\text{P}\{^1\text{H}\}$ NMR (d_8 -THF): δ -67.8 (s). Combustion data for recrystallized material were consistently low in carbon. A crown ether derivative (**7**) was prepared for crystallographic confirmation of the nature of **6**.

Preparation of [K(18-crown-6)(THF)₂][1,8-(TrippP)₂C₁₄H₁₀] (**7**). A flask was charged with **6** (53.5 mg, 0.0671 mmol) and 18-crown-6 (78.2 mg, 0.296 mmol). Et₂O (2 mL) was transferred to the reaction vessel, resulting in a colour change of the mixture from brown to black. Within minutes of initiating the reaction, the formation of an insoluble black oil was observed. The resulting mixture was allowed to stand at ambient temperature for 4 h, and then was concentrated under vacuum to give a dark red solid. A crystal of this product suitable for X-ray diffraction analysis was grown from a mixture of THF–pentane at $-35\text{ }^{\circ}\text{C}$. No further characterisation of the product was undertaken.

Preparation of 1,3-(^tBuPLiCH₂)₂C₆H₄·TMEDA (8**)**. An aliquot of ⁿBuLi (1.86 mL, 1.73 M in hexanes, 3.22 mmol) was added dropwise *via* syringe to a solution of **2** (455 mg, 1.61 mmol) in toluene (40 mL) at $0\text{ }^{\circ}\text{C}$. The resulting cloudy pale yellow mixture was warmed to ambient temperature, and TMEDA (0.48 mL, 3.20 mmol) was added *via* syringe, affording a cloudy orange solution that was stirred for 1 h. Subsequent removal of the volatiles under vacuum yielded a yellow-orange solid, which was washed with pentane ($3 \times 2\text{ mL}$) to liberate **8** as a yellow powder (588.4 mg, 89%, m.p. $170\text{ }^{\circ}\text{C}$ (dec., gradually darkens and loses crystallinity above $140\text{ }^{\circ}\text{C}$)). ^1H NMR (C_6D_6): δ 7.96 (br s, 1H, aromatic 2-*H*), 7.19 (br s, 1H overlapping with $\text{C}_6\text{D}_5\text{H}$ signal, aromatic 5-*H*), 7.13 (br m, 2H,

aromatic 4,6-*H*), 3.21 (br s, 4H, *CH*₂P), 2.16 (br s, 12H, (CH_3)₂N CH_2)₂), 1.92 (br s, 4H, (CH_3)₂N CH_2)₂), 1.54 (br s, 18H, C(CH_3)₃). $^{13}\text{C}\{^1\text{H}\}$ NMR (C_6D_6): δ -151.2 (br s, aromatic 1,3-*C*), 130.5 (br s, aromatic 5-*C*), 123.5 (br s, aromatic 4,6-*C*), 57.9 (br s, (CH_3)₂N CH_2)₂), 47.6 (br s, (CH_3)₂N CH_2)₂), 35.6 (br s, C(CH_3)₃), 30.1 (br s, C(CH_3)₃), 9.0 (br m, *CH*₂P). The aromatic 2-*C* resonance was obscured by the solvent signal. $^{31}\text{P}\{^1\text{H}\}$ NMR (C_6D_6): δ -0.5 (br s). Anal. Calcd (%) for C₂₂H₄₂N₂Li₂P₂: C: 64.38; H: 10.31; N: 6.83 found: C: 64.05; H: 10.22; N: 6.63. X-ray quality single crystals of **8** were grown from a concentrated solution of the complex in pentane at $-35\text{ }^{\circ}\text{C}$.

X-ray crystallography

A suitable crystal of each compound was coated in hydrocarbon oil and mounted on a glass fibre. Data were collected at 173 K with ω and φ scans on a Bruker Apex II diffractometer using Mo K α ($\lambda = 0.71073\text{ \AA}$) radiation with Bruker SMART software.³⁵ The unit cell parameters were calculated and refined from the full data set. Crystal cell refinement and data reduction were carried out using the Bruker APEX 2 and SAINT programs.³⁶ After reduction, the data were corrected for absorption based on equivalent reflections using SADABS.³⁷ Structures were solved by direct methods with SHELXS-97 and refinement was carried out on F^2 against all independent reflections by the full-matrix least squares method by using the SHELXL-97 program.³⁸ Hydrogen atoms were calculated geometrically and isotropically refined as riding models to their parent atoms, with the exception of the P–H hydrogen atoms of (MesPH)₂C₁₄H₈, (TrippPH)₂C₁₄H₁₀·0.5(C₆H₆) and 4·2 (solvent), which were located on the difference Fourier map and refined freely. In the case of (MesPH)₂C₁₄H₈, two regions of electron density were found close to each P atom, indicating possible proton disorder. The larger of the two peaks in each case was assigned as the P–H proton, and no disorder modeling was attempted. All non-hydrogen atoms were refined with anisotropic thermal parameters except in certain cases of disorder (*vide infra*). Thermal ellipsoid plots were generated using OLEX2.³⁹ Crystallographic data are summarised in Table 1. Special considerations were required for the refinement of (TrippPH)₂C₁₄H₁₀·0.5(C₆H₆), 4·2(solvent) and **7**, discussed in the following sections.

For (TrippPH)₂C₁₄H₁₀·0.5(C₆H₆), one triisopropylphenyl ring (C30, 73%/C30B, 27%) and one isopropyl group (C21, 71%/C21B, 29%) were disordered. A geometric constraint was applied in order to obtain reasonable bond distances and angles in the triisopropylphenyl ring. The more abundant component of the disordered regions was refined anisotropically, while the minor component was held isotropic.

The unit cell of the diselenide 4·2(solvent) contained heavily disordered solvent molecules (either of isoelectronic pentane or diethyl ether) for which no suitable model could be found. The electron density associated with these molecules was removed from the reflection data using the program SQUEEZE (PLATON).⁴⁰ After this treatment, two voids of ca. 411 \AA^3 remained in the unit cell, each originally containing 155 electrons and corresponding to ca. four solvent molecules.

Table 1 Crystal data for compounds (MesPH)₂C₁₄H₈, 4·2(solvent), (TrippPH)₂C₁₄H₁₀·0.5(C₆H₆), 7, and 8

| Crystal | 1b | 4·2(solvent) ^b | (TrippPH) ₂ C ₁₄ H ₁₀ ·0.5(C ₆ H ₆) | 7·2(C ₄ H ₈ O) | 8 |
|--|---|---|---|--|---|
| Empirical formula | C ₃₂ H ₃₂ P ₂ | C ₂₆ H ₅₂ P ₂ Se ₂ | C ₄₇ H ₆₁ P ₂ | C ₉₂ H ₁₅₂ K ₂ O ₁₈ P ₂ | C ₄₄ H ₈₄ Li ₄ N ₄ P ₄ |
| Formula mass | 478.52 | 584.56 | 687.90 | 1686.35 | 820.79 |
| Colour, habit | Orange, prism | Colourless, rod | Colourless, prism | Orange, plate | Yellow, prism |
| Crystal dimensions (mm) | 0.66 × 0.25 × 0.13 | 0.36 × 0.16 × 0.06 | 0.42 × 0.10 × 0.06 | 0.66 × 0.39 × 0.05 | 0.60 × 0.20 × 0.20 |
| Crystal system | Monoclinic | Monoclinic | Monoclinic | Triclinic | Monoclinic |
| Space group | <i>P</i> 2 ₁ / <i>n</i> | <i>P</i> 2 ₁ / <i>c</i> | <i>C</i> 2/ <i>c</i> | <i>P</i> 1 | <i>P</i> 2 ₁ / <i>n</i> |
| <i>Z</i> | 4 | 4 | 8 | 2 | 4 |
| <i>a</i> (Å) | 8.447(1) | 9.251(1) | 33.518(3) | 13.310(2) | 16.370(1) |
| <i>b</i> (Å) | 26.236(2) | 21.756(2) | 15.037(1) | 17.990(3) | 19.895(1) |
| <i>c</i> (Å) | 11.855(1) | 12.731(1) | 16.596(2) | 21.542(3) | 17.438(1) |
| α (°) | 90 | 90 | 90 | 87.891(2) | 90 |
| β (°) | 93.140(1) | 90.930(6) | 97.155(1) | 87.743(2) | 113.083(1) |
| γ (°) | 90 | 90 | 90 | 68.936(2) | 90 |
| Collection ranges | −10 ≤ <i>h</i> ≤ 10, −33 ≤ <i>k</i> ≤ 33, −15 ≤ <i>l</i> ≤ 15 | −11 ≤ <i>h</i> ≤ 10, −18 ≤ <i>k</i> ≤ 24, −12 ≤ <i>l</i> ≤ 15 | −39 ≤ <i>h</i> ≤ 39, −17 ≤ <i>k</i> ≤ 17, −19 ≤ <i>l</i> ≤ 19 | −15 ≤ <i>h</i> ≤ 15, −21 ≤ <i>k</i> ≤ 21, −25 ≤ <i>l</i> ≤ 25 | −19 ≤ <i>h</i> ≤ 19, −22 ≤ <i>k</i> ≤ 23, −20 ≤ <i>l</i> ≤ 20 |
| Volume (Å ³) | 2623.2(3) | 2562.1(4) | 8299.2(13) | 4808.3(12) | 5224.56(17) |
| <i>D</i> _{calcd} (g cm ^{−3}) | 1.212 | 1.515 | 1.101 | 1.165 | 1.044 |
| Absorption coeff. (μ) (mm ^{−1}) | 0.184 | 3.004 | 0.135 | 0.194 | 0.175 |
| <i>F</i> (000) | 1016 | 1224 | 2984 | 1672 | 1792 |
| θ range for data collection (°) | 1.89–27.10 | 2.86–25.03 | 1.88–25.03 | 1.64–25.03 | 2.58–25.03 |
| Observed reflections | 36 816 | 29 577 | 49 571 | 58 552 | 40 844 |
| Independent reflections [<i>R</i> _{int}] | 5785 [0.0211] | 4432 [0.0561] | 7324 [0.0678] | 16 947 [0.0556] | 922 [0.0414] |
| Data/restraints/parameters | 5785/0/321 | 4432/0/195 | 7324/0/522 | 16 947/42/1028 | 9222/0/525 |
| Goodness-of-fit on <i>F</i> ² | 1.037 | 1.006 | 1.017 | 1.028 | 1.020 |
| Final <i>R</i> indices [<i>I</i> > 2σ(<i>I</i>)] ^a | <i>R</i> ₁ = 0.0460, <i>wR</i> ₂ = 0.1215 | <i>R</i> ₁ = 0.0378, <i>wR</i> ₂ = 0.0834 | <i>R</i> ₁ = 0.0529, <i>wR</i> ₂ = 0.1168 | <i>R</i> ₁ = 0.0642, <i>wR</i> ₂ = 0.1624 | <i>R</i> ₁ = 0.0435, <i>wR</i> ₂ = 0.1010 |
| <i>R</i> indices, all data ^a | <i>R</i> ₁ = 0.0538, <i>wR</i> ₂ = 0.1271 | <i>R</i> ₁ = 0.0598, <i>wR</i> ₂ = 0.0886 | <i>R</i> ₁ = 0.0967, <i>wR</i> ₂ = 0.1404 | <i>R</i> ₁ = 0.1122, <i>wR</i> ₂ = 0.1805 | <i>R</i> ₁ = 0.0696, <i>wR</i> ₂ = 0.1153 |
| Largest diff. peak and hole (e Å ^{−3}) | 0.448 and −0.510 | 0.647 and −0.366 | 0.325 and −0.516 | 0.892 and −0.627 | 0.363 and −0.270 |

^a $R_1 = \sum ||F_o| - |F_c|| / \sum |F_o|$, $wR_2 = [\sum w(F_o^2 - F_c^2)^2 / \sum wF_o^4]^{1/2}$. ^b The solvent is one of either isoelectronic pentane or diethyl ether; it has been arbitrarily defined as pentane (see Experimental for details).

In the refinement of 7, one triisopropylphenyl ring (C15, 65%/C15B, 35%) and one THF ligand (O8, 75%/O8B, 25%) were disordered and some restraints were applied. The more abundant component of the disordered regions was refined anisotropically, while the minor component was held isotropic. The structure contained two severely disordered THF solvent molecules in the asymmetric unit, for which no suitable model could be found. The electron density associated with the disordered regions was removed from the reflection file using the program SQUEEZE (PLATON),⁴⁰ leaving a void of ca. 645 Å³.

Conclusion

We have presented protocols for the synthesis and characterisation of two secondary diphosphines, as well as their metallation by group 1 reagents to yield diphosphido complexes. These compounds are potential supporting ligands for rare transition metal coordination complexes featuring two phosphido donors. Furthermore, C–H activation in addition to deprotonation of 1a–b and 2 could provide access to trianionic ligands for stabilization of high-valent d- or f-block metal complexes. Further studies into the reactivity of the reported alkali metal diphosphido salts, as well as those with modified ligand frameworks, with transition metal halides will be the subject of a subsequent report.

Acknowledgements

The authors acknowledge the Natural Sciences and Engineering Research Council (NSERC), Alberta Ingenuity (New Faculty Award for PGH), the Canada Foundation for Innovation, the University of Lethbridge, and the University of Winnipeg for financial support, and Dr Craig A. Wheaton for elemental analyses.

References

- 1 C. J. Moulton and B. L. Shaw, *J. Chem. Soc., Dalton Trans.*, 1976, 1020.
- 2 For example, see the following reviews: (a) M. Albrecht and G. van Koten, *Angew. Chem., Int. Ed.*, 2001, **40**, 3750; (b) J. I. van der Vlugt and J. N. H. Reek, *Angew. Chem., Int. Ed.*, 2009, **48**, 8832.
- 3 (a) M. Gupta, C. Hagen, R. J. Flesher, W. C. Kaska and C. M. Jensen, *Chem. Commun.*, 1996, 2083; (b) C. M. Jensen, *Chem. Commun.*, 1999, 2443.
- 4 C. Gunanathan, Y. Ben-David and D. Milstein, *Science*, 2007, **317**, 790.
- 5 (a) P. Brooks, D. C. Craig, M. J. Gallagher, A. D. Rae and A. Sarroff, *J. Organomet. Chem.*, 1987, **323**, C1; (b) P. Brooks, M. J. Gallagher and A. Sarroff, *Aust. J. Chem.*, 1987, **40**,

- 1341; (c) D. M. Anderson, P. B. Hitchcock, M. F. Lappert and I. Moss, *Inorg. Chim. Acta*, 1988, **141**, 157.
- 6 D. M. Anderson, P. B. Hitchcock, M. F. Lappert, W. P. Leung and J. A. Zora, *J. Organomet. Chem.*, 1987, **333**, C13.
- 7 O. Walter, T. Klein, G. Huttner and L. Zsolnai, *J. Organomet. Chem.*, 1993, **458**, 63.
- 8 R. P. Davies, M. G. Martinelli, L. Patel and A. J. P. White, *Inorg. Chem.*, 2010, **49**, 4626.
- 9 D. W. Stephan, *Angew. Chem., Int. Ed.*, 2000, **39**, 314.
- 10 J. Ellermann and F. Poersch, *Angew. Chem., Int. Ed. Engl.*, 1967, **6**, 355.
- 11 H. Köpf and V. Richtering, *J. Organomet. Chem.*, 1988, **346**, 355.
- 12 N. P. Mankad, E. Rivard, S. B. Harkins and J. C. Peters, *J. Am. Chem. Soc.*, 2005, **127**, 16032.
- 13 M. Mazzeo, M. Lamberti, A. Massa, A. Scettri, C. Pellicchia and J. C. Peters, *Organometallics*, 2008, **27**, 5741.
- 14 M. Mazzeo, M. Lamberti, I. D'Auria, S. Milione, J. C. Peters and C. Pellicchia, *J. Polym. Sci., Part A: Polym. Chem.*, 2010, **48**, 1374.
- 15 I. D'Auria, M. Mazzeo, D. Pappalardo, M. Lamberti and C. Pellicchia, *J. Polym. Sci., Part A: Polym. Chem.*, 2011, **49**, 403.
- 16 M. Mazzeo, M. Strianese, O. Köhl and J. C. Peters, *Dalton Trans.*, 2011, **40**, 9026.
- 17 R. C. Bauer, Y. Gloaguen, M. Lutz, J. N. H. Reek, B. de Bruin and J. I. ver der Vlugt, *Dalton Trans.*, 2011, **40**, 8822.
- 18 I. D'Auria, M. Lamberti, M. Mazzeo, S. Milione, G. Roviello and C. Pellicchia, *Chem.–Eur. J.*, 2012, **18**, 2349.
- 19 M. C. MacInnis, R. McDonald and L. Turculet, *Organometallics*, 2011, **30**, 6408.
- 20 L. Turculet and R. McDonald, *Organometallics*, 2007, **26**, 6821.
- 21 M. S. Winston and J. E. Bercaw, *Organometallics*, 2010, **29**, 6408.
- 22 J. Koller, S. Sarkar, K. A. Abboud and A. S. Veige, *Organometallics*, 2007, **26**, 5438.
- 23 P. E. Romero, M. T. Whited and R. H. Grubbs, *Organometallics*, 2008, **27**, 3422.
- 24 T. W. Lyons, D. Guironnet, M. Findlater and M. Brookhart, *J. Am. Chem. Soc.*, 2012, **134**, 15708.
- 25 M. W. Haenel, S. Oevers, J. Bruckmann, J. Kuhnigk and C. Krüger, *Synlett*, 1998, 301.
- 26 J. B. Lambert and J.-H. So, *J. Org. Chem.*, 1991, **56**, 5960.
- 27 D. L. Haire, E. G. Janzen, V. J. Robinson and I. Hrvoic, *Magn. Reson. Chem.*, 2004, **42**, 835.
- 28 F. Dornhaus, H.-W. Lerner and M. Bolte, *Acta Crystallogr., Sect. E: Struct. Rep. Online*, 2007, **63**, o4917.
- 29 D. Julienne, K. R. D. Johnson and P. G. Hayes, unpublished results, 2009.
- 30 A. Bondi, *J. Phys. Chem.*, 1964, **68**, 441.
- 31 C. L. Hilton and B. T. King, *Organometallics*, 2006, **25**, 4058.
- 32 J. J. Brooks, W. Rhine and G. D. Stucky, *J. Am. Chem. Soc.*, 1972, **94**, 7346.
- 33 F. Dornhaus, M. Bolte, H.-W. Lerner and M. Wagner, *J. Organomet. Chem.*, 2007, **692**, 2949.
- 34 (a) Ar = Tripp: C. Frenzel, F. Somoza, S. Blaurock and E. Hey-Hawkins, *J. Chem. Soc., Dalton Trans.*, 2001, 3115; (b) Ar = Mes: G. W. Rabe, G. P. A. Yap and A. L. Rheingold, *Inorg. Chem.*, 1997, **36**, 1990.
- 35 APEX 2, *Crystallography software package*, Bruker AXS Inc., Madison, WI, 2005.
- 36 SAINT, *Data Reduction Software*, Bruker AXS, 1999.
- 37 G. M. Sheldrick, *SADABS v.2.01, Area Detector Absorption Correction Program*, Bruker AXS, Madison, WI, 1998.
- 38 G. M. Sheldrick, *Acta Crystallogr., Sect. A: Fundam. Crystallogr.*, 2008, **64**, 112.
- 39 O. V. Dolomanov, L. J. Bourhis, R. J. Gildea, J. A. K. Howard and H. Puschmann, *J. Appl. Crystallogr.*, 2009, **42**, 339.
- 40 P. Van Sluis and A. L. Spek, *Acta Crystallogr., Sect. A: Fundam. Crystallogr.*, 1990, **46**, 194.